Networks and Heterogeneous Media

NHM, 20(3): 782–797.
DOI: 10.3934/nhm.2025033
Received: 07 April 2025
Revised: 30 May 2025
Accepted: 06 June 2025
Published: 07 July 2025

https://www.aimspress.com/journal/NHM

Research article

The low inter-radiator transmittance MIMO antenna with DGS and parasitic elements for Ku-Band application

Muhammad Irshad Khan[1,*], Muhammad Kabir Khan[2], Saeed Ur Rahman[3], Ahmad Mubarak[1], Abdul Basit[4], Ehab Seif Ghith[5], Shimaa A. Hussien[6], Mostafa Rashdan[7] and Mohammad Salman[7]

[1] School of electronics and information engineering, Wuxi University, Wuxi 214105, China
[2] College of electronics and information engineering, Nanjing University of Aeronautics and Astronautics (NUAA), Nanjing 211106, China
[3] School of electronic engineering, Xidian University, Xi'an China
[4] Department of Electrical Engineering, University of Engineering and Technology Peshawar, Pakistan
[5] Department of Mechatronics, Faculty of Engineering, Ain shams University, Cairo 11566, Egypt
[6] Electrical Engineering Department, Princess Nourah Bint Abdulrahman University, P.O. Box 84428, Riyadh 11671, Saudi Arabia
[7] College of Engineering and Technology, American University of the Middle East, Egaila 54200, Kuwait

* **Correspondence:** Email: 100031@cwxu.edu.cn.

Abstract: This article presents a four-port multiple-input multiple-output (MIMO) antenna using double-sided decoupling techniques. The size of the quad-element MIMO antenna is 36 mm × 36 mm × 1.6 mm. The reflection coefficient is <−10 dB and the transmittance is <−27 dB in the range of 14 to 18 GHz, with a total impedance bandwidth of 4 GHz. Parasitic elements and a defected ground structure (DGS) are used to reduce the inter-radiator transmittance. Parasitic elements are used on the top side of the antenna to minimize transmittance between neighboring elements. DGS is used on the back side to minimize transmittance in both neighboring elements and diagonal elements. The envelope correlation coefficient (ECC) is <0.0075, the diversity gain (DG) is >9.96 dB, and the peak gain is 5.75 dBi. The presented antenna was analyzed in terms of the reflection coefficients (Sij ∈ i = j), transmittance (Sij ∈ i ≠ j), ECC, multiplexing efficiency, DG, and peak gain. Additionally, the design was tested in an anechoic chamber. The proposed design is an acceptable candidate for Ku-band applications after experimental investigations.

Keywords: MIMO; parasitic elements; DG; ECC; DGS; transmittance and gain

1. Introduction

In today's high data rate with low latency, minimal multipath fading, an improved channel capacity, and an enhanced transmission quality with low transmitting power are needed for modern communication systems [1]. MIMO antennas have recently gained more attention. The single antenna is replaced with printed MIMO antennas to increase the data rate, improve the channel capacity, enhance the transmission quality, and reduce multipath fading without consuming more bandwidth and transmitting power [2]. Commonly, satellite communication is line-of-sight, and MIMO antennas are installed on both the transmitting and receiving sides to enhance the transmission quality and channel capacity. The MIMO antenna system has a significant contribution to the aforementioned challenges, though there are also some limitations. For example, placing multiple antennas in close proximity can lead to strong mutual coupling, while deploying antennas with large distances between them increases the circuit size. Tackling these challenges is the main goal of the proposed design.

Various techniques have been used in MIMO antennas for decoupling, such as decoupling stub [3], a self-isolating MIMO arrangement [4], a split-ring resonator (SRR) [5], meta-material [6], a dielectric resonator [7], parasitic elements [8], neutralizing lines [9], complementary SRR [10], and a DGS [11]. The authors of [8] presented a trapezoidal-shaped quad-port antenna, with a volume of 50 mm × 50 mm × 1.6 mm, an isolation of >25 dB, and an ECC of <0.04. In [9], the authors presented a dual-port design with a neutralizing line; the size of the prototype was 21 mm × 34 mm × 1.6 mm, the isolation was >22 dB, and the ECC was <0.005. The authors of [10] suggested a MIMO antenna with a complementary SRR, a volume of 60 mm × 60 mm × 1.6 mm, an ECC <0.4, and a transmittance of −22 dB. In [11], the authors reported a quad-port antenna with a very large size of 74 mm × 74 mm × 1.524 mm, an isolation of >34 dB, and an ECC of <0.001. In [12], the authors suggested a quad ports antenna with an overall size of 50 mm × 50 mm × 0.8 mm; inter digital capacitors and SRR were used to isolate elements, with a transmittance <−20 dB and an ECC below 0.01. In [13], the authors suggested a two element circular shape MIMO antenna with reflectors for X and Ku band applications, a volume of 28 mm × 16 mm × 1.6 mm, an isolation >26 dB, and an ECC <0.04. In [14], the authors suggested a quad port MIMO antenna with dimensions of 65.8 mm × 45 mm × 1.68 mm; meandering techniques were used for decoupling, with an isolation of >35 dB and an ECC of <0.005. In [15], the authors suggested a two-port MIMO antenna with horn shape radiating elements; the size of the design was 15 mm × 25 mm × 1.6 mm, the transmission coefficient was <−20 dB, and the ECC was <0.02. In [16], the authors suggested a dendritic meandered shape quad-port MIMO antenna with slot lines; the size of antenna was 84 mm × 26 mm × 1.6 mm, with isolations of 15, 28, and 16 dB on the presented bands. In [17], the authors suggested a tri-bands quad-port Minkowiski-modified Fractal shape MIMO antenna with a large size of 68.4 mm × 52 mm × 1.6 mm, an ECC <0.07, a DG >9.96 dB, and an isolation >26 dB. In [18], the presented fractal shape two-port MIMO antenna had a volume of 25 mm × 35 mm × 1.6 mm, DGS was used for isolation, had an ECC <0.052 and a DG >9.98. In [19], the authors designed a two-port MIMO antenna with a T-shape decoupling stub, a volume of 18 mm × 36 mm × 1.6 mm, mutual coupling <−20 dB, and an ECC <0.05. The authors of [20], presented two-port CPW-fed antenna, with a volume of 18 mm × 22 mm × 1.6 mm, an ECC <0.07, isolation >20 dB, and a DG >9.97 dB. In [21], the authors suggested a two-port MIMO antenna with large size of 45 mm ×

70 mm × 1.6 mm, an ECC <0.004, a DG >9.15, and isolation >22 dB. In [22], the authors reported a two-port MIMO antenna with a very large size of 33.5 mm × 25 mm × 3.5 mm, an isolation of >20 dB, and an ECC of <0.015. In [23], the authors presented a quad-port design with a parasitic element and a DGS; the size of the prototype was 30 mm × 30 mm × 0.8 mm, with an isolation of >27 dB, and an ECC of <0.001. The authors of [24] suggested a MIMO antenna with a loop parasitic element; the volume of the design was 55 mm × 55 mm × 1.6 mm, with an ECC <0.022 and a transmittance of −22 dB. The authors of [25] reported a quad-element MIMO antenna with a DGS for isolation, an overall size of 110 μm × 110 μm, a DG of almost 10 and an ECC of almost zero. The authors of [26] reported a quad-element design for various bands communication; the size of the antenna was 60 mm× 60 mm, with an isolation of about 50 dB, a DG of almost 10 dB, and an ECC near to zero. In [27], the authors reported a quad-port terahertz design with an isolation of 30 dB, a size of 130 μm × 130 μm × 1.6 μm, an ECC <0.2, and a DG >8.2 dB. In [28], the authors reported two-port design with I-shape ground for isolation, a DG greater than 9.90 dB, and an ECC <0.05 in given band. In [29], the authors reported a two-port meta-material base MIMO antenna for 6 G and WiMAX applications; the size of the antenna was 112 mm × 26.5 mm, the CCL was <0.35, a DG >9.97 dB, an ECC was less than 0.18, and the TARC was less than –9.97 dB.

The stop-band filters and metasurface-based absorbers are also used for decoupling. The authors of [30] reported a dual-port ring-shaped antenna with a band-stop filter; the volume of the design was 31 mm × 31 mm × 0.8 mm, with an isolation >25 dB and an ECC <0.05. The authors of [31] presented a two-port design with a size of 100 mm × 50 mm × 0.8 mm. Absorbers are used for isolation, with ECC <0.5 and isolation >23 dB. The authors of [32] reported a dual-port MIMO design with a volume of 18 mm × 36 mm × 1.6 mm, with an ECC <0.1, a DG >9.95 dB, and an isolation >18 dB. The authors of [33] suggested a four-port tapered CPW-fed MIMO antenna with a volume of 63 mm × 63 mm × 1.6 mm, with ECC <0.01 and isolation >17 dB. The authors suggested a simple square-shaped MIMO antenna with an Electromagnetic Soft Surface. The overall size of the suggested antenna was 41.05 mm × 24.55 mm × 1.6 mm, with an isolation >17 dB [34]. In [35], the authors suggested a two-port square-shaped antenna with square parasitic elements. The volume of the design was 55 mm × 41 mm, with an isolation >26 dB. In [36], the authors presented a two-port ring-shaped antenna with a volume of 25 mm × 32 mm × 0.8 mm, mutual coupling <−15 dB, an ECC of <0.04, and a peak gain of >1.23 dBi. In [37], the authors reported a quad-port MIMO antenna, DGS is used for decoupling, ECC <0.006, and DG >9.99 dB. Similarly, in [38], the authors also presented a four-port design for various band communications with DGS for isolation, with an ECC equal to 0.11 and a DG >8.87 dB. A comparison of the presented design for Ku-band applications with most relevant articles are presented in Table 1.

In the above literature, mostly two-port antennas with large sizes, low isolation, and complex structures due to the decoupling techniques are presented. The authors mostly calculated the DG and ECC from S-parameters, which is a less precise method compared to the far-field radiation pattern. Furthermore, some authors presented multi-port MIMO antennas without connected grounds. Keeping the above-mentioned issues in mind, the authors suggested a MIMO antenna with quad elements, a connected ground, and novel decoupling techniques for satellite communication. The radiating patches are placed orthogonal to each other and fed with inset feeding. The parasitic elements and DGS are introduced to increase the isolation. The parasitic elements are designed on the front side to isolate neighboring elements, and DGS are used on the back side to isolate diagonal elements.

Table 1. Comparison of MIMO antenna for Ku-band application with cited literature.

Ref.	Size (mm × mm)	Ports	Isolation (dB)	ECC	Peak Gain (dBi)	DG (dB)	CCL (bits/sec/Hz)	MEG (dB)
[8]	50 × 50	4	>25	<0.04	3	>9.96	---	---
[9]	21 × 34	2	>22	<0.005	5.22	>9.99	0.26	-6
[10]	60 × 60	4	>22	<0.4	---	---	---	---
[12]	50 × 50	4	>20	<0.01	---	---	---	---
[13]	28 × 16	2	>26	<0.04	5.8	>9.99	0.2	-3
[14]	65.8 × 45	4	>35	<0.005	5.35	---	---	---
[15]	15 × 25	2	>20	<0.02	3	>9.99	---	---
[16]	84 × 26	4	>15	---	---	---	---	---
[17]	68.4 × 52	4	>26	<0.07	---	>9.96	---	---
[18]	25 × 35	2	>69	<0.052	---	>9.98	0.00015	0.9
[19]	18 × 36	2	>20	<0.05	4	9.8	--	--
[20]	18 × 22	2	>20	<0.07	5	9.97	---	---
[21]	45 × 70	2	>22	<0.004	7.37	>9.15	0.25	8.1
[22]	33.5 × 25	2	>20	<0.015	---	---	---	---
This work	36 × 36	4	>27	<0.0075	5.75	9.96	0.2	-3

2. Antenna design and configuration

The proposed MIMO antenna for Ku-band applications is designed on a 1.6 mm thick FR4 material. The overall dimensions of the quad-element MIMO antenna is 36 mm × 36 mm × 1.6 mm. The presented MIMO antenna consists of four radiating elements, four slots of DGS, and parasitic elements. Furthermore, each radiating element is designed from half circular and rectangular patches. The dimensions of single element antenna is 14 mm × 14 mm × 1.6 mm, the radius 'r_p' is equal to 5 mm, the dimensions of the rectangular patch '$l_p \times w_p$' is equal to 3.6 mm × 7 mm, and the dimensions of the feed line '$l_f \times w_f$' is equal to 5.25 mm × 1.6 mm. The dimension of the slot '$l_{slot} \times w_{slot}$' is 1.8 mm × 5.6 mm; the remaining dimensions are given in Table 2. The evaluation mechanism and their results of the radiating patch are depicted in Figures 1 and 2, respectively. The lower frequency of the impedance bandwidth is adjusted by using rectangular patch, and a slot is used to widen the impedance bandwidth, which is justified from Figure 2. The radius is calculated from Eqs (1) and (2) [39], where 'a' is the radius of the circular patch, $'f_o'$ is the resonance frequency, $'\varepsilon_r'$ is the relative permittivity, and 'h' is the height of the substrate:

$$a = \frac{F}{\left\{1+\frac{2h}{\pi\varepsilon_r F}\left[\ln\left(\frac{\pi F}{2h}\right)+1.7726\right]\right\}^{1/2}}, \tag{1}$$

$$F = \frac{8.791\times10^9}{f_o\sqrt{\varepsilon_r}}. \tag{2}$$

The single radiating element is expanded to the quad-elements and placed orthogonally to each other. The quad-elements antenna without a decoupling structure is shown in Figure 3(a). The S11 is almost the same, and the transmittance is −16 dB, as shown in Figure 3(b). Parasitic elements and the

DGS are added to minimize the transmittance and to increase isolation. Decoupling structures are used to disturb the field distribution. Parasitic elements are introduced to the center of each side on the top layer of the design to minimize the transmittance between neighboring elements. All the parasitic elements are similar in structure, and their size is '$l_s \times w_s$' 13 mm × 1 mm. The design of a quad-port MIMO antenna for Ku-band application with parasitic elements is depicted in Figure 4(a). The transmittance of neighboring elements is minimized from −16 to −22 dB, as clearly shown in Figure 4(b). The DGS is introduced to the center of each side on the bottom to form a flower-shaped ground plane. The DGS minimizes the transmittance for both neighboring elements and diagonal elements. The size of each DGS is '$l_d \times w_d$' 13 mm × 4 mm. The quad-port antenna with a DGS and their results are depicted in Figure 5. The overall transmittance is minimized from −16 to −24 dB. The presented quad-port MIMO antenna for Ku-band communication is achieved by merging parasitic elements and a DGS, as depicted in Figure 6. The S_{11} is almost the same in all designs, and the transmittance is minimized to −27 dB in the presented design, as justified from Figure 7.

Additionally the isolation mechanism is analyzed in terms of the current distribution, as illustrated in Figure 8. For a better understanding, element-2 and element-4 are excited both with and without decoupling techniques. It is clearly shown in Figure 8(a) that the current is transferred to the remaining three ports, such as port-1, port-3, and port-4, without decoupling techniques; in this situation, isolation is minimal, and the transmittance is very high from port-2 to the other ports. In Figure 8(b), the current is concentrated on radiating element-2, parasitic elements, and the DGS. In this situation, the current is coupled to the parasitic elements and the DGS, and the transmittance is low among the ports. Similarly, in Figure 8(c), the density of the current is found on non-excited elements such as port-1, port-2, and port-3. In this situation, isolation is minimal, and the transmittance is very high from port-4 to the other ports. In Figure 8(d), the current is concentrated on element-4, parasitic elements, and the DGS. In this situation, the current is coupled to the parasitic elements and the DGS: thus, the transmittance is minimal, and isolation is high among the ports. The radiating patches have the same shape, size, and symmetry, so some of the S-parameters are same (e.g., $S_{12} = S_{21}$, $S_{13} = S_{31}$, $S_{23} = S_{32}$, $S_{24} = S_{42}$, $S_{34} = S_{43}$, $S_{14} = S_{41}$, $S_{11} = S_{22} = S_{33} = S_{44}$).

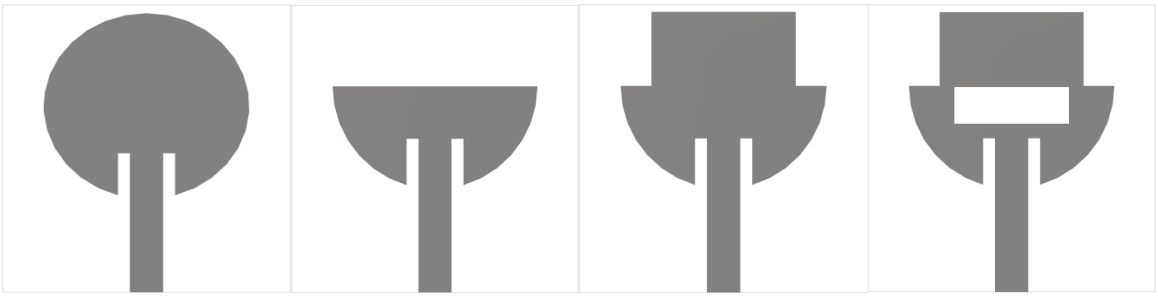

(a) (b) (c) (d)

Figure 1. Design evaluation of radiating element: (a) Stage-1; (b) Stage-2; (c) Stage-3; (d) Proposed.

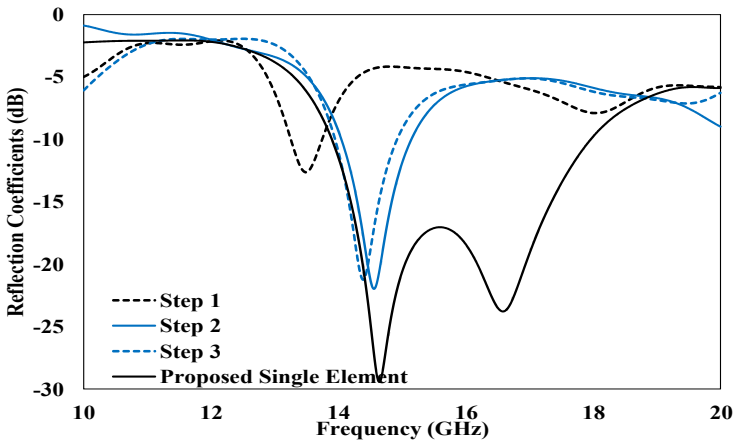

Figure 2. Results of design evaluation stages of a single element.

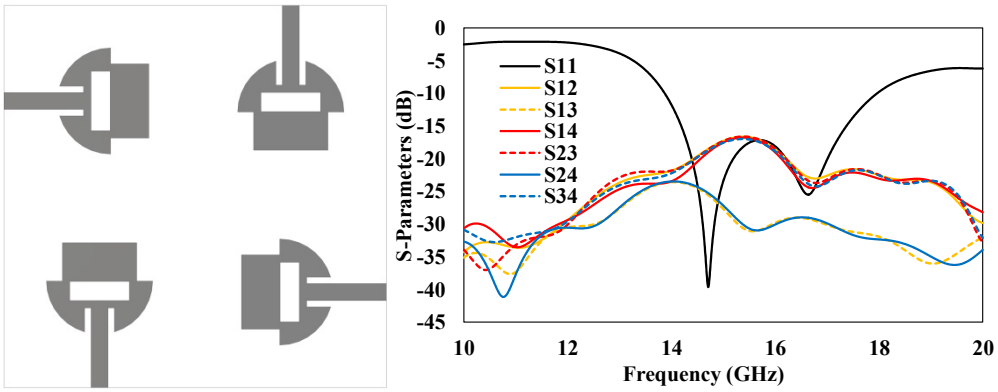

(a) (b)

Figure 3. Proposed MIMO antenna without decoupling techniques: (a) Design; (b) S-Parameters.

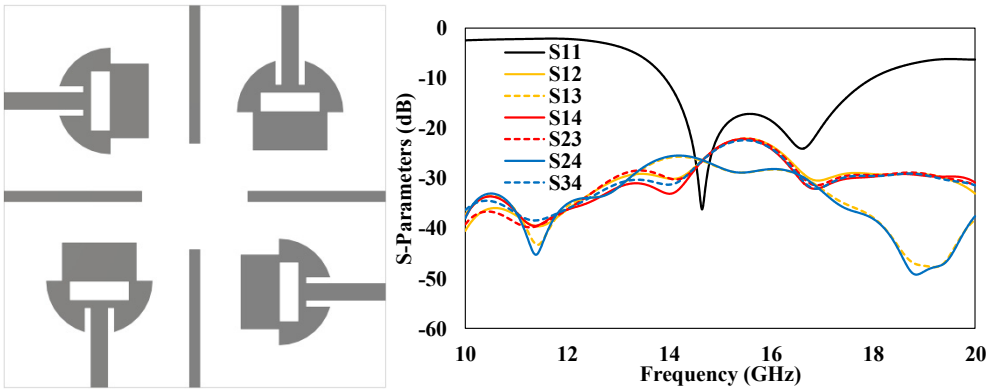

(a) (b)

Figure 4. MIMO antenna with parasitic elements: (a) Design; (b) S-Parameters.

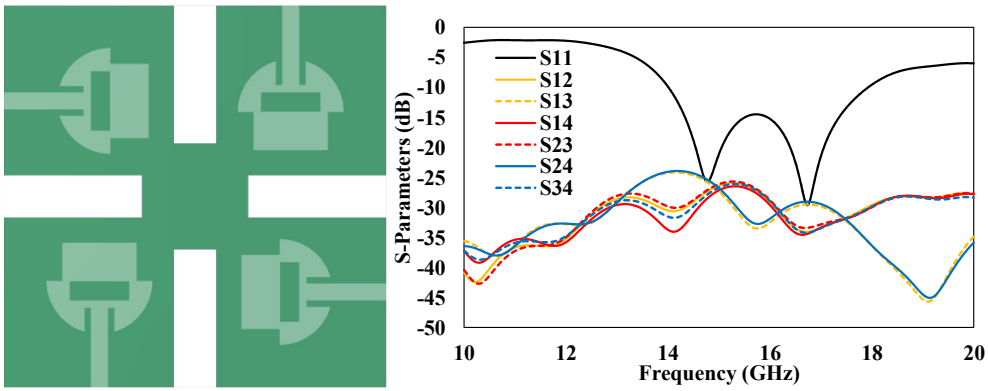

(a) (b)

Figure 5. MIMO antenna with a DGS: (a) Design; (b) S-Parameters.

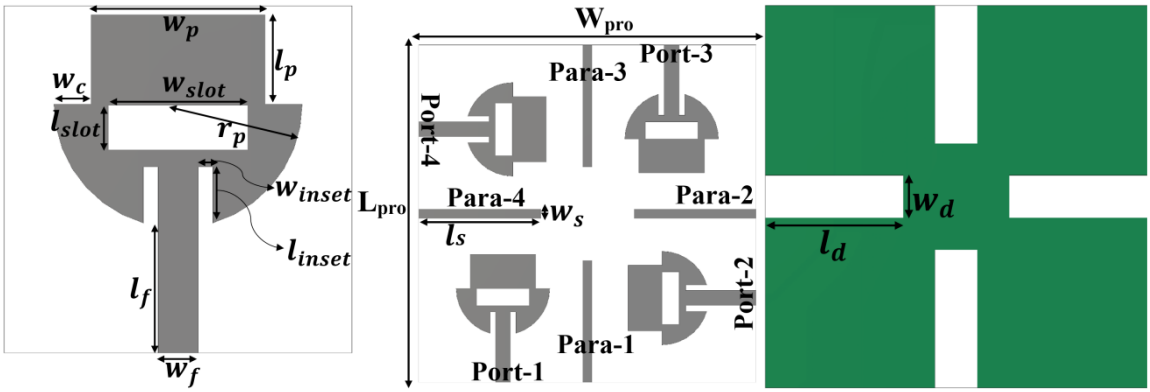

(a) (b) (c)

Figure 6. Presented MIMO antenna for Ku-band applications: (a) Single element Design; (b) Front side; (c) Back side.

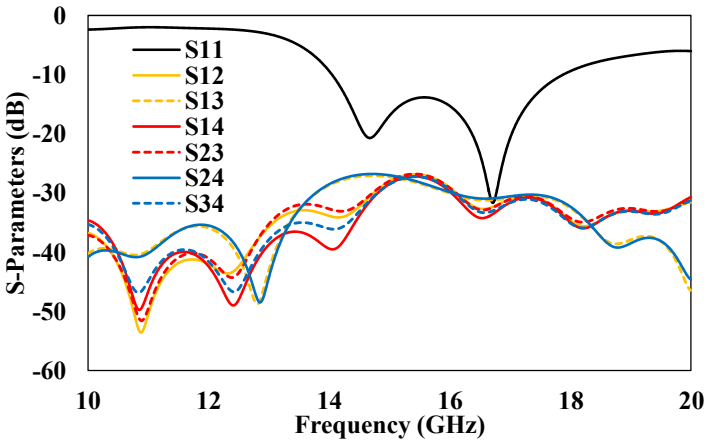

Figure 7. S-Parameters of the presented design for Ku-band applications.

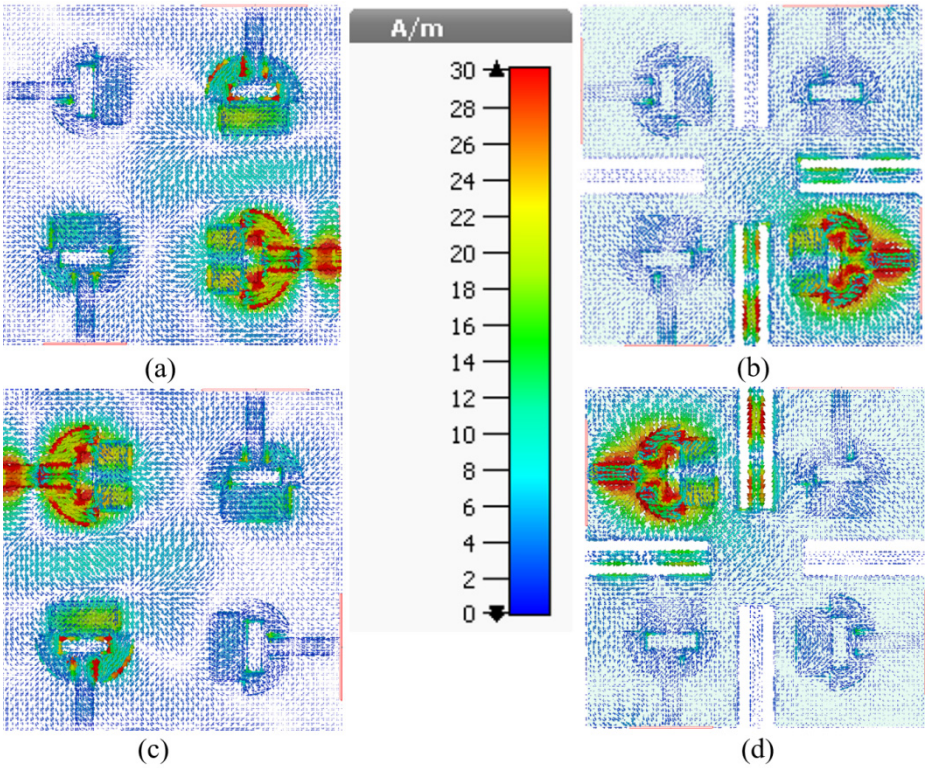

Figure. 8. Surface current distribution of the presented MIMO antenna for Ku-band applications at 16 GHz: (a) without decoupling structure (element-2 excited); (b) with parasitic element and DGS (element-2 excited); (c) without decoupling techniques (element-4 excited); (d) with parasitic element and DGS (element-4 excited)

Table 2. Dimensions parameters of presented MIMO antenna for Ku-band application.

Parameters	Value (mm)	Parameters	Value (mm)
W_{pro}	36	L_{pro}	36
w_{inset}	0.6	l_{inset}	2.25
w_s	1	l_s	13
w_d	4	l_d	13
w_c	1.5	r_p	5

3. Results

The proposed MIMO antenna for satellite communication is optimized in the Computer Simulation Technology (CST) Studio and fabricated using a 1.6 mm thick FR4 material. The top and bottom views of the presented design are depicted in Figure 9. The experimentally tested and simulated results are illustrated in Figure 10. The experimentally tested and simulated reflection coefficient was <-10 dB and the transmittance was <-27 dB in the range of 14 to 18 GHz with a bandwidth of 4 GHz. The tested and simulated XZ-plane ($\phi = 0$, E-plane) and YZ-plane ($\phi = 90$, H-plane) radiation pattern at 15 and 16.5 GHz frequencies are shown in Figure 11. The main lobe radiation in the XZ-plane at 15 GHz is observed at 300° to 330° and 30° to 60°, and the minimum radiation occurred at 135° and 200°. Similarly in YZ-plane, the main lobe radiation is observed at 30° and the minimum

radiation occurred at 170°, as shown in Figure 11(a). The main lobe radiation in both the XZ-plane and the YZ-plane at 16.5 GHz are noted at 330°. In the XZ-plane, minimum radiation is noted at 150° and 180°; similarly, in the YZ-plane, minimum radiation is noted at 120°, which is clearly justified from Figure 11(b). Additionally, the co-polar and cross-polar components are shown in Figure 12: The cross-polar components are <−20 dB and the co-polar components are much higher than the cross-polar components.

The diversity performance is characterized in terms of the ECC, DG, and multiplexing efficiency; for an uncorrelated MIMO antenna, with values of ECC = 0 and DG = 10 dB, the ECC must be <0.5. Similarly, the DG is greater than 8.66 dB in a practical design. The ECC and DG are calculated from Eqs (3) and (4) [40]:

$$ECC = \frac{\left|\iint_{4\pi}[\vec{F_i}(\theta,\phi)\blacksquare\vec{F_j}(\theta,\phi)]d\Omega\right|^2}{\iint_{4\pi}\left|\vec{F_i}(\theta,\phi)\right|^2 d\Omega \iint_{4\pi}\left|\vec{F_j}(\theta,\phi)\right|^2 d\Omega}, \tag{3}$$

$$DG = 10\sqrt{1-(\mathrm{ECC})^2}, \tag{4}$$

where $\vec{F_i}(\theta,\phi)$ and $\vec{F_j}(\theta,\phi)$ are the far-field radiation due to the i^{th} port and j^{th} port, respectively, and ■ is the Hermitian product. The ECC <0.0075 and DG >9.96 dB, as clearly shown in Figure 13. Generally, the multiplexing efficiency is considered as the total efficiency, but practically, it consists of a correlation and efficiency imbalance. The multiplexing efficiency is <−2 dB, which is lower than the radiation efficiency, as shown in Figure 14. The simulated and measured peak gain, which are nearly the same and equal to 5.75 dBi, are also illustrated in Figure 13. Moreover, the diversity performance is investigated in terms of the total active reflection coefficient (TARC). The TARC is investigated at various angles from Eq (5) [41], and illustrated in Figure 15. The TARC is <−10 dB in the given Ku-band bandwidth for all angles. Additionally, the diversity performance is characterized in terms of the channel capacity loss (CCL) and the mean effective gain (MEG) in MIMO antennas. For good communication, the satisfactory value of the CCL is 0.5 bits/sec/Hz, and the MEG should be less than −3 dB. The MEG and CCL are calculated from Eqs (6) and (7) [42]: The CCL is <0.2 bits/sec/Hz and the MEG <−3 dB in the given Ku-band, as illustrated in Figure 16.

$$TARC = \frac{\sqrt{\sum_{k=0}^{n}(|b_k|^2)}}{\sqrt{\sum_{k=0}^{n}(|a_k|^2)}}, \tag{5}$$

$$CCL = -\log_2 \det(\varphi^R), \tag{6}$$

$$MEGi = 0.5\left(1-\sum_{j=1}^{k}\left|S_{ij}\right|^2\right), \tag{7}$$

where $|b_k|$ *and* $|a_k|$ are exciting and scattering vectors, respectively, and φ^R is the correlation matrix.

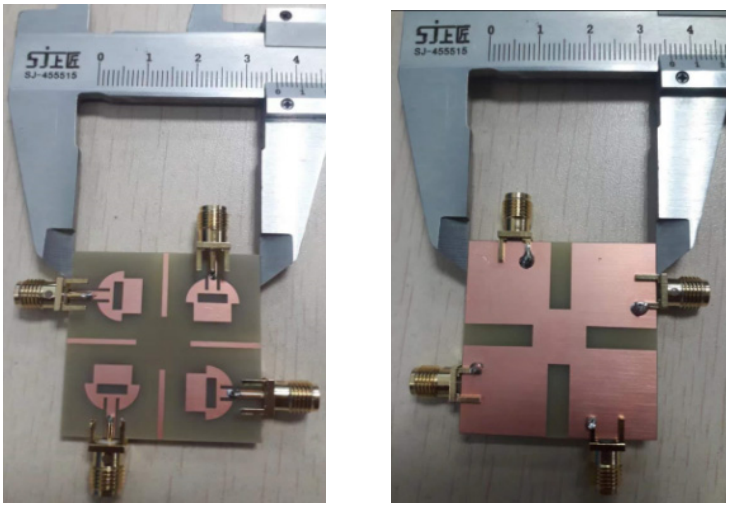

(a) (b)

Figure 9. Prototype of the presented MIMO antenna for Ku-band applications: (a) Top view; (b) bottom view.

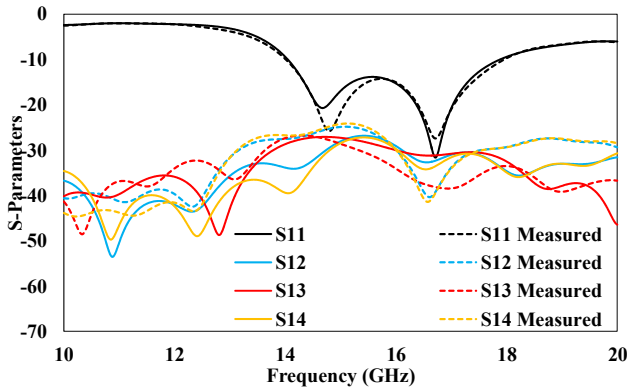

Figure 10. S-parameters of the presented MIMO antenna for Ku-band applications.

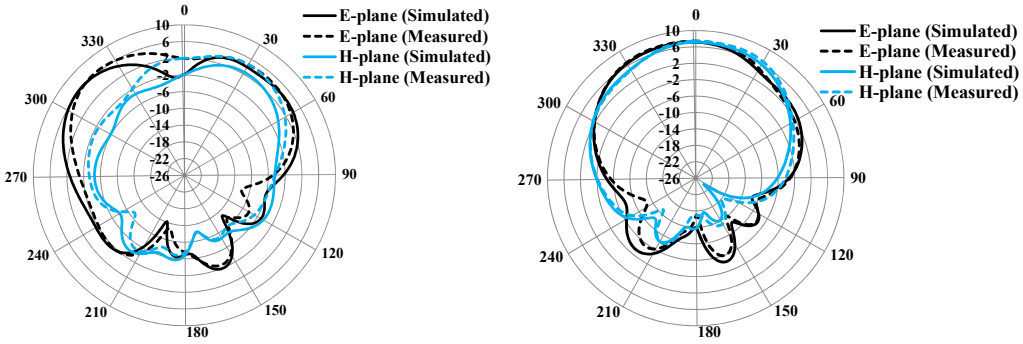

(a) (b)

Figure 11. Radiation pattern of the presented MIMO antenna: (a) 15 GHz; (b) 16.5 GHz.

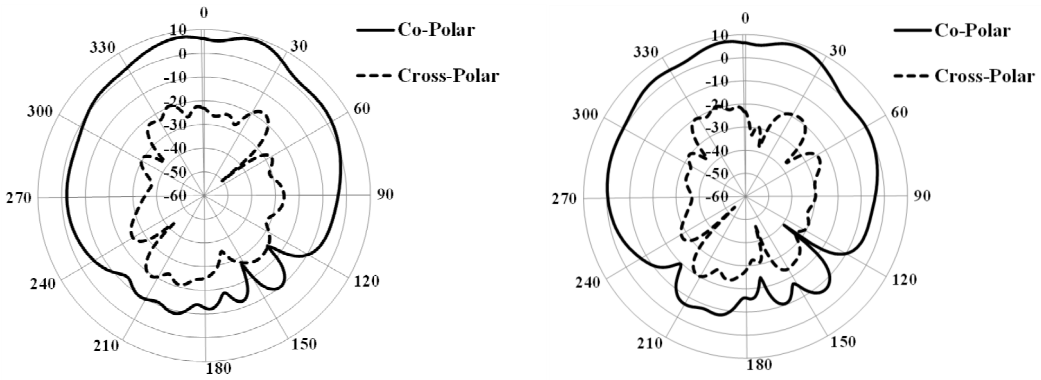

Figure 12. Co and cross polarization of the presented MIMO antenna: (a) 15 GHz; (b) 16.5 GHz.

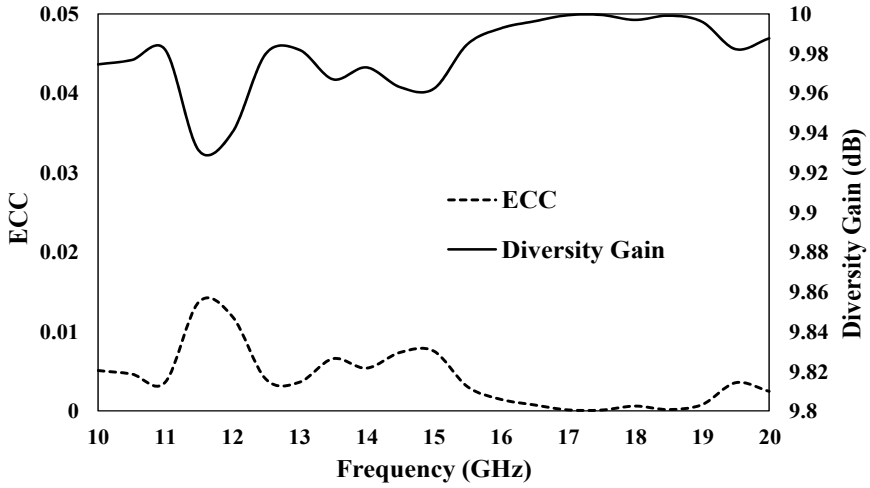

Figure 13. ECC and DG of the presented MIMO antenna for Ku-band applications.

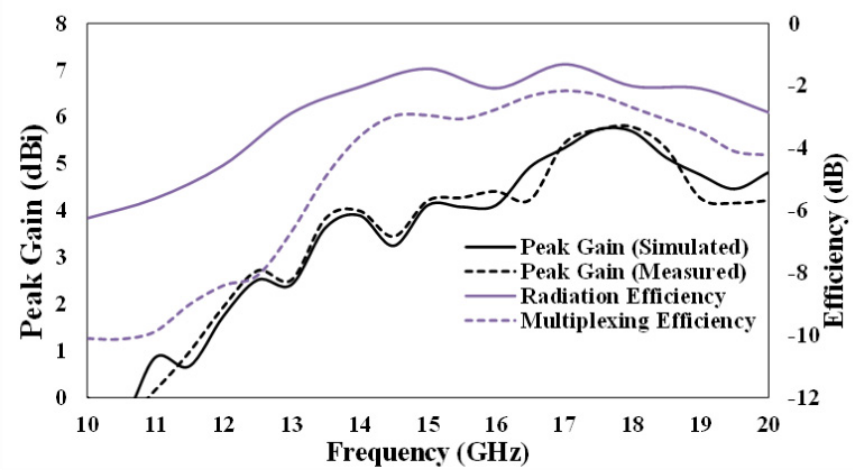

Figure 14. Peak gain and Multiplexing efficiency of the MIMO antenna for Ku-band applications.

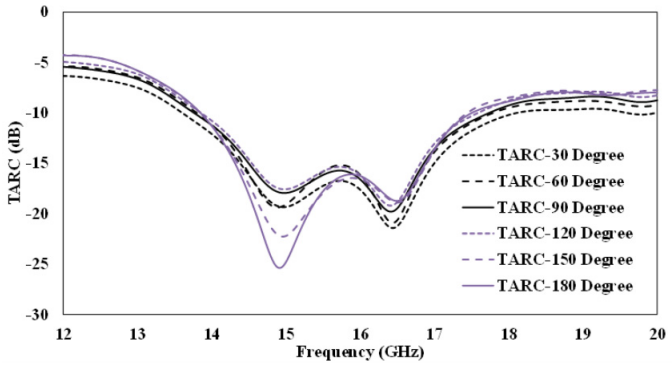

Figure 15. TARC of the MIMO antenna for Ku-band applications.

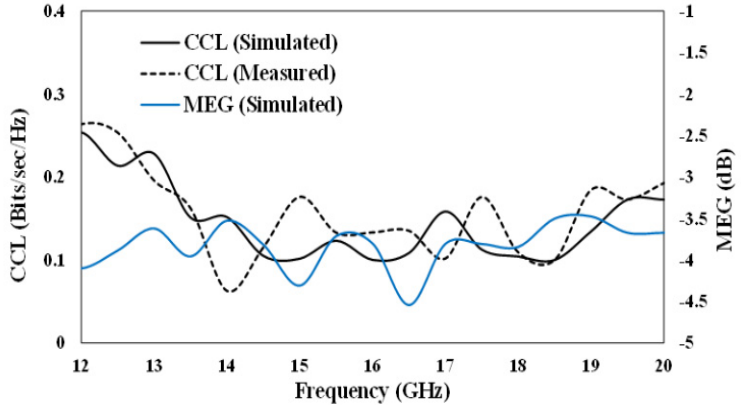

Figure 16. CCL and MEG of the MIMO antenna for Ku-band applications.

4. Conclusions

In this article, an MIMO Antenna for Ku-band applications was proposed. The antenna was designed on a 1.6 mm thick FR4 material. Parasitic elements were printed on the front side to minimize the transmittance between neighbor elements, and the DGS was used on the back side to minimize the transmittance for both neighbor elements and diagonal elements. The reflection coefficient was <−10 dB and the transmittance was <−27 dB in the range of 14 to 18 GHz, with a total impedance bandwidth of 4 GHz. The ECC <0.0075, DG >9.96 dB, and Peak gain was 5.75 dBi. The presented design is an acceptable candidate for Ku-band applications after experimental investigations of the multiplexing efficiency, ECC, S-parameters, DG, and peak gain.

Authors contribution

Conceptualization: Muhammad Irshad Khan. Investigation: Muhammad Irshad Khan. Methodology: Muhammad Irshad Khan, Muhammad Kabir Khan. Software: Muhammad Irshad Khan. Supervision: Ehab seif Ghith, Shimaa A.Hussien. Validation: Muhammad Irshad Khan, Mostafa Rashdan, Mohammad Salman. Writing—original draft: Muhammad Irshad Khan, Writing—review & editing: Muhammad Irshad Khan, Muhammad Kabir Khan, Saeed Ur Rahman Abdul Basit, Ahmad Mubarak, Mostafa Rashdan, Mohammad Salman.

Use of AI tools declaration

The authors declare they have not used Artificial Intelligence (AI) tools in the creation of this article.

Acknowledgments

This research was funded by Princess Nourah bint Abdulrahman University Researchers Supporting Project number (PNURSP2025R827), Princess Nourah bint Abdulrahman University, Riyadh, Saudi Arabia.

Conflict of interest

The authors declare that they have no known competing financial interests or personal relationships that could have appeared to influence the work reported in this paper.

References

1. T. S. P. See, Z. N. Chen, An ultrawide band diversity antenna, *IEEE Trans. Antennas Propag.,* **57** (2009), 1597–1605. https://doi.org/10.1109/TAP.2009.2019908
2. M. Sharma, A. K. Gautam, N. Agrawal, N. Singh, Design of MIMO planar antenna at 24 GHz band for radar, communication and sensors applications, *AEU Int. J. Electron. Commun.,* **136** (2021), 153747. https://doi.org/10.1016/j.aeue.2021.153747
3. M. I. Khan, M. I. Khattak, S. U. Rahman, A. B. Qazi, A. A. Telba, A. Sebak, Design and investigation of modern UWB-MIMO antenna with optimized isolation, *Micromachines*, **11 (**2020), 432. https://doi.org/10.3390/mi11040432
4. J. Joseph, G. S. Let, C. B. Pratap, A compact wideband self-isolated uniplanar quad MIMO antenna for C-band applications, *Phys. Scr.*, **99** (2024), 045513. https://doi.org/10.1088/1402-4896/ad302e
5. P. Kansal, A. K. Mandpura, N. Kumar, Investigation of circularly polarized MIMO antenna with enhanced isolation for sub-6 GHz application, *Phys. Scr.*, **99** (2024), 105536. https://doi.org/10.1088/1402-4896/ad7651
6. Y. Li, H. Yang, H. Cheng, J. Wu, Y. Yang, S. Li, et al., Design and analysis of metasurface-based CPW-Fed UWB MIMO antenna for wireless communication systems, *Phys. Scr.*, **98** (2023), 095510. https://doi.org/10.1088/1402-4896/acec1e
7. Y. Rai, A. Sharma, S. Agarwal, R. Gupta, Circularly polarized dielectric resonator based MIMO antenna for sub-6 GHz 5G cognitive radio applications, *Phys. Scr.*, **99** (2024), 065547. https://doi.org/10.1088/1402-4896/ad4ad4
8. M. H. Reddy, D. Sheela, A. Swaminath, A four port circularly polarized printed multiple input multiple-output antenna with enhanced isolation, *Int. J. Commun. Syst.,* **35** (2022), e5061. https://doi.org/10.1002/dac.5061
9. R. N. Tiwari, P. Singh, B. K. Kanaujia, A compact UWB MIMO antenna with neutralization line for WLAN/ISM/mobile applications, *Int. J. RF Microwave Comput. Aided Eng*., **29 (**2019), e21907. https://doi.org/10.1002/mmce.21907

10. A. Ramachandran, S. V. Pushpakaran, M. Pezholil, V. Kesavath, A four-port MIMO antenna using concentric square-ring patches loaded with CSRR for high isolation, *IEEE Antennas Wirel. Propag. Lett.,* **15** (2015), 1196–1199. https://doi.org/10.1109/LAWP.2015.2499322
11. M. A. Sufian, N. Hussain, A. Abbas, J. Lee, S. G. Park, N. Kim, Mutual coupling reduction of a circularly polarized MIMO antenna using parasitic elements and DGS for V2X communications, *IEEE Access,* **25** (2022), 56388–56400. https://doi.org/10.1109/ACCESS.2022.3177886
12. D. Sarkar, A. Singh, K. Saurav, K. V. Srivastava, Four element quad-band multiple-input-multiple-output antenna employing split-ring resonator and inter-digital capacitor, *IET Microw. Antennas Propag.*, **9** (2015), 1453–1460. https://doi.org/10.1049/iet-map.2015.0189
13. T. Addepalli, V. R. Anitha, Compact two-port MIMO antenna with high isolation using parasitic reflectors for UWB, X and Ku band applications, *Prog. Electromagn. Res. C.,* **102** (2020), 63–77. https://doi.org/10.2528/PIERC20030402
14. W. J. Wu, Y. F. Cheng, G. Wang, Isolation enhancement for four-element MIMO antenna by using novel meandering technique, *Microw. Opt. Technol. Lett.,* **64** (2022), 1434–1441. https://doi.org/10.1002/mop.33296
15. M. I. Khan, M. I. Khattak, M. I. Al-Hasan, Miniaturized MIMO antenna with low inter-radiator transmittance and band rejection features, *J. Electromagn. Eng. Sci.*, **21** (2021), 307–315. https://doi.org/10.26866/jees.2021.4.r.38
16. Y. Liu, A novel four-port high isolation MIMO antenna design for high-capacity wireless applications, *Microw. Opt. Technol. Lett.,* **60** (2018), 1476–1481. https://doi.org/10.1002/mop.31189
17. P. B. Saha, R. K. Dash, D. Ghoshal, Triple-band four-port MIMO antenna with reduced mutual coupling using Minkowiski-modified novel fractal loop, *Wirel. Pers. Commun.,* **117** (2021), 2253–2271. https://doi.org/10.1007/s11277-020-07970-3
18. G. N. J. Sree, S. Nelaturi, Opportunistic control of fractal-based MIMO antenna for sub-6-GHz 5G applications, *Int. J. Commun. Syst.,* **34** (2021), e4991. https://doi.org/10.1002/dac.4991
19. M. I. Khan, M. I. Khattak. Designing and analyzing a modern MIMO-UWB antenna with a novel stub for stop band characteristics and reduced mutual coupling, *Microw. Opt. Technol. Lett.*, **62** (2020), 3209–3214. https://doi.org/10.1002/mop.32425
20. M. I. Khattak, M. I. Khan, M. A. Anab, M. Al-Hasan, J. Nebhen, Miniaturized CPW-fed UWB-MIMO antennas with decoupling stub and enhanced isolation, *Int. J. Microw. Wirel. Technol.,* **14** (2021), 456–464. https://doi.org/10.1017/S1759078721000556
21. L. Ma, Z. Shao, J. Lai, C. Gu, J. Mao, Bandwidth enhancement of H-plane MIMO patch antennas in integrated sensing and communication applications, *IEEE Open J. Antennas Propag.,* **5** (2023), 90–103. https://doi.org/10.1109/OJAP.2023.3334219
22. L. Ma, Z. Shao, J. Lai, C. Gu, J. Mao, A compact dual-decoupling scheme for aperture-coupled and probe-fed closely spaced wideband microstrip antennas, *IEEE Trans. Antennas Propag.,* **71** (2023), 9072–9077. https://doi.org/10.1109/TAP.2023.3306637
23. M. I. Khan, M. K. Khan, S. U. Rahman, M. Anab, A. Basit, Quad ports millimeter-wave MIMO antenna with parasitic element and defected ground structure for radar sensing application, *Radio Sci.,* **60** (2025), e2024RS008174. https://doi.org/10.1029/2024RS008174

24. M. I. Khan, S. Liu, S. U. Rahman, M. K. Khan, M. Sajjad, A. Basit, et al., Electromagnetic coupling suppression of circularly polarized mimo antenna with novel loop parasitic for UWB communication, *Analog Integr. Circ. Sig. Process.,* **118** (2024), 577–588. https://doi.org/10.1007/s10470-024-02256-1
25. K. P. Shobhit, D. Jansari, H. M. Almawgani, Design and optimization of meandered plasmonic MIMO antenna with defected ground structure showing ultra-wideband response and high isolation for 6G/TWPAN communication, *Opt. Quantum Electron.,* **56** (2024), 86. https://doi.org/10.1007/s11082-023-05633-8
26. K. N. Devi, C. Annadurai, I. Nelson, S. Lavadiya, Novel-shaped expandable quad-port MIMO antenna using FR4 material with features of high isolation and band width for 5G networks, Wi-Fi, and satellite communication applications, *Opt. Quantum Electron.,* **56** (2024), 1272. https://doi.org/10.1007/s11082-024-07232-7
27. G. Dhandapani, S. Lavadiya, S. Aldosary, Fractal-shaped super UWB (96 THz) of quadpot MIMO antenna for 6G communication, *Opt. Quantum Electron.,* **56** (2024), 1613. https://doi.org/10.1007/s11082-024-07416-1
28. S. Lavadiya, T. Kamani, D. Jansari, Plasmonics antenna design using a metamaterial-based resonating structure with I-shaped ground for 5G communication, *Plasmonics,* **19** (2024), 3101–3118. https://doi.org/10.1007/s11468-024-02222-7
29. J. P. Siyara, M. N Jiyani, O. Alsalman, S. P Lavadiya, Novel metamaterial array-based dual port MIMO antenna using low profile substrate with feature multiband, and high isolation for sub-6G, IoT, and WiMAX applications, *Phys. Scr.*, **99** (2024), 095531. https://doi.org/10.1088/1402-4896/ad6b59
30. C. Prashant, K. Ravi, K. Ashwani, P. Kamlesh, K. Anand, High isolation pattern diversity multiband MIMO antenna using ring and stub with bandstop filter, *Int. J. Electron.,* **110** (2023), 2064–2084. https://doi.org/10.1080/00207217.2022.2129814
31. V. Puri, H. S. Singh, Design of an isolation improved MIMO antenna using metasurface based absorber for wireless applications, *Optik*, **259 (**2022), 168963. https://doi.org/10.1016/j.ijleo.2022.168963
32. S. Kareemulla, V. Kumar, Diversity performance of band notched ultra-wideband MIMO antenna. *Optik*, **272 (**2023), 170128. https://doi.org/10.1016/j.ijleo.2022.170128
33. D. K. Raheja, B. K Kanaujia, S. Kumar, Low profile four-port super-wideband multiple-input-multiple-output antenna with triple band rejection characteristics, *Int. J. RF Microwave Comput. Aided Eng.,* **29** (2019), e21831. https://doi.org/10.1002/mmce.21831
34. K. S. Banerjee, S. Mandal, S. Banerjee, Reduction of mutual coupling and cross-polarization of microstrip MIMO antenna using Electromagnetic Soft Surface (EMSS), *Radio Sci.,* **57** (2022), e2021RS007377. https://doi.org/10.1029/2021RS007377
35. H. H. Tran, N. Hussain, H. C. Park, N. T. Nguyen, Isolation in dual-sense CP MIMO antennas and role of decoupling structures, *IEEE Antennas Wirel. Propag. Lett.,* **21** (2022), 1203–1207. https://doi.org/10.1109/LAWP.2022.3161669
36. X. Cao, Y. Xia, L. Wu, H. Zhang, Q. Zeng, Two-port ring shaped MIMO antenna with quad-band, *Int. J. RF Microwave Comput. Aided Eng.,* **31** (2021), e22782. https://doi.org/10.1002/mmce.22782

37. T. Doloi, Trishna, G. S. Das, P. P. Kalita, A. Buragohain, A novel 4-port MIMO antenna with chamfered edge for 5G NR n77/n78/n79 bands and WLAN applications, *Phys. Scr.*, **99** (2024), 105013. https://doi.org/10.1088/1402-4896/ad723e
38. R. K. Mistri, S. K. Mahto, A. K. Singh, R. Sinha, Quad element MIMO antenna for C, X, Ku, and Ka-band applications, *Sensors,* **23** (2023), 8563. https://doi.org/10.3390/s23208563
39. C. A. Balanis, Antenna theory: Analysis and design, 3rd ed. Hoboken, NJ, USA: Wiley, 2005, 811–820. Available from: https://bcs.wiley.com/he-bcs/Books?action=index&bcsId=8129&itemId=047166782X.
40. S. Blanch, J. Romeu, I. Corbella, Exact representation of antenna system diversity performance from input parameter description, *Electron. Lett.,* **39** (2003), 705–707. https://doi.org/10.1049/el:20030495
41. M. Manteghi, Y. R. Samii, Multiport characteristics of a wideband cavity backed annular patch antenna for multi polarization operations, *IEEE Trans. Antennas Propag.,* 53 (2005), 466–74. https://doi.org/10.1109/TAP.2004.838794
42. A. A. Megahed, M. Abdelazim, E. H. Abdelhay, H. Y. M. Soliman, Sub-6 GHz highly isolated wideband MIMO antenna arrays, *IEEE Access*, **10** (2022), 19875–19889. https://doi.org/10.1109/ACCESS.2022.3150278

AIMS Press